Optimum Design on Lobe Shapes of Gerotor Oil Pump

J. H. Kim
ERC/NSDM at Pusan National University,
30 Changjeon-dong, Kumjeong-Ku, Pusan 609-735, Korea
Chul Kim*
Research Institute of Mechanical Technology at Pusan National University,
30 Changjeon-dong, Kumjeong-Ku, Pusan 609-735, Korea
Y. J. Chang
School of Mechanical Engineering at Pusan National University,
30 Changjeon-dong, Kumjeong-Ku, Pusan 609-735, Korea

A gerotor pump is suitable for oil hydraulics of machine tools, automotive engines, compressors, constructions and other various applications. In particular the pump is an essential machine element that feeds lubricant oil in an automotive engine. The subject of this paper is the theoretical analysis of internal lobe pump whose the main components are the two rotors. Usually the outer one is characterized by lobes with a circular shape, while the inner rotor profile is determined as a conjugate to the other. For this reason the first topic presented here is the definition of the geometry of the rotors starting from the design parameters. The choice of these parameters is subject to some limitations in order to limit the pressure angle between the rotors. Now we will consider the design optimization. The first step is the determination of the instantaneous flow rate as a function of the design parameter. This allows us to calculate three performance indexes commonly used for the study of positive displacement pumps: the flow rate irregularity, the specific flow rate, and the specific slipping. These indexes are used to optimize the design of the pump and to obtain the sets of optimum design parameter. Results obtained from the analysis enable the designer and manufacturer of the oil pump to be more efficient in this field.

Key Words: Cusp, Lobe Shape, Pressure Angle, Specific Slipping

1. Introduction

An oil pump is an essential part in the operation of an automotive engine. It changes the mechanical energy of the engine into pressure or velocity energy of engine oil so that it feeds lubricant oil into the parts of engine to prevent lobe wear or the adherence of the parts. The gerotor pump with its inner and outer rotors is simple and compact and is highly accurate due to the development of the sintering process, although the shape of the lobes is complex. And it has small fluctuation and good performance for suction in the long term because of the small relative motion between the rotors.

The gerotor pump with less noise than the other types is being used in driving the force of supply in lubricant oil or pressure for a transmission's oil. The co-ordinates of inner rotor are obtained by simulating the contact points of the two rotors. A chamber between two subsequent pairs of lobes in mesh is calculated by Colbourne (1975). The lobe of the outer rotor with a circular shape is

* Corresponding Author,
E-mail: chulki@pusan.ac.kr
TEL: +82-51-510-2489; **FAX**: +82-51-512-9835
Research Institute of Mechanical Technology at Pusan National University, 30 Changjeon-dong, Kumjeong-Ku, Pusan 609-735, Korea. (Manuscript **Received** January 6, 2006; **Revised** June 20, 2006)

determined by Sae-gusa (Saegusa et al., 0000) as rotating the outer rotor to separate the next points in the inner rotor reference system, while the inner rotor is always obtained as its conjugate. Recently, Tsay has determined the co-ordinates of an inner rotor by simulating the cutting process (Tsay and Yu, 1989; Yu and Tsay, 1990). Also Kim et. all (2006) suggested a new method to derive the close-form equation of trochoidal gerotor pump. On the basis of this approach, an integrated system to generate loci of the inner and outer rotor, of contact points and rotation simulation, and flow rate and its irregularity for the rotor profile was constructed.

This study carried out a geometrical and kinematic analysis considering design variables and design limits of outer rotor with a circular lobe shape. Through the analysis, the design limit area that does not present cusps and loops was found and the specific slipping related to the pressure angle and wear was calculated in the design limit area. The study obtained the optimal design parameters by fixing the lobe numbers z_1 and z_2 and calculating flow rate and flow rate irregularity according to d/e and r_{t2}/e.

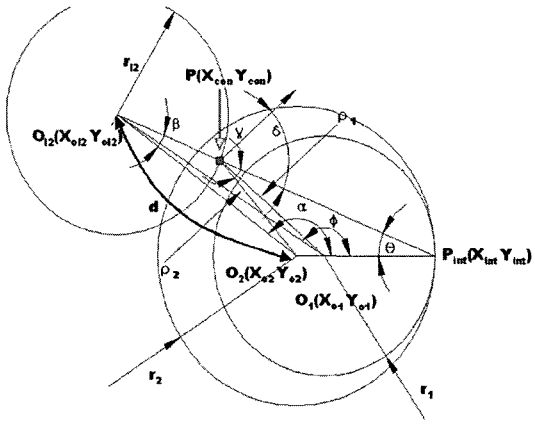

Fig. 1 Conjugated profile tracing

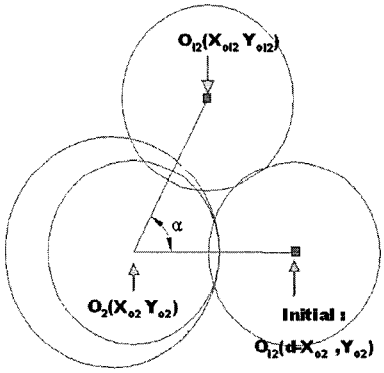

Fig. 2 Center of curvature in the rotated position

2. Gerotor Geometry and Kinematics

2.1 Inner and outer rotors

The outer rotor is made of z_2 lobes whose profile is an arc of circumference centered in O_{t2} and with radius r_{t2} as shown in Fig. 1. The pitch curve is the circumference with a radius equal to r_2 in Fig. 1. The geometrical parameters that allow us to completely define the outer rotor are the number of lobes z_2, the radius of curvature r_{t2}, the distance d between the center of curvature O_{t2}, the center of the outer rotor O_2 and the pitch radius r_2.

$$z_2=z_1+1,\ r_1=ez_1,\ r_2=ez_2 \tag{1}$$

So, in a reference system $x_2O_2y_2$ the inner rotor center O_1 is at a distance equal to r_2/z_2 from O_2 and we can put O_1 on the positive x_2 axis for convenience. A second reference system is taken with origin in O_1, which is useful to determine the equations that describe the inner rotor lobe.

For a finite rotation of an outer rotor α', the coordinate of the center of the curvature circle is expressed as Eq. (2) in Fig. 2.

$$\begin{pmatrix} X_{ot2} \\ Y_{ote} \end{pmatrix}=\begin{pmatrix} \cos\alpha & -\sin\alpha \\ \sin\alpha & \cos\alpha \end{pmatrix}\begin{pmatrix} d \\ 0 \end{pmatrix}+\begin{pmatrix} X_{o2} \\ Y_{o2} \end{pmatrix} \tag{2}$$

At this time, the contact point p is able to be calculated in Eq. (3).

$$\overrightarrow{O_{t2}P}=\frac{\overrightarrow{O_{t2}P_{\text{int}}}}{|O_{t2}P_{\text{int}}|}\times r_{t2} \tag{3}$$

The inner rotor profile is obtained by calculating geometrical parameters as increasing of rotated angle. A point on the inner rotor profile, P_{in} (x_{in}, y_{in}), is expressed as follows

$$\begin{pmatrix} X_{\text{in}} \\ Y_{\text{in}} \end{pmatrix}=\begin{pmatrix} \cos\theta_{z1} & -\sin\theta_{z1} \\ \sin\theta_{z1} & \cos\theta_{z1} \end{pmatrix}\begin{pmatrix} X_{con}-X_{o1} \\ Y_{con}-Y_{ol} \end{pmatrix}+\begin{pmatrix} X_{ol} \\ Y_{o1} \end{pmatrix} \tag{4}$$

where θ_{z1} is expressed as shown in Eq. (5).

$$\frac{\theta_{z1}}{\theta_{z2}}=\frac{z_1}{z_2},\ \theta_{z2}=z_2\alpha' \tag{5}$$

The outer rotor profile is obtained in the same way. A point on the outer rotor profile, P_{out} (x_{out}, y_{out}), is expressed as Eq. (6).

$$\begin{pmatrix}X_{\text{out}}\\ Y_{\text{out}}\end{pmatrix}=\begin{pmatrix}\cos\theta_{z2} & -\sin\theta_{z2}\\ \sin\theta_{z2} & \cos\theta_{z2}\end{pmatrix}\begin{pmatrix}X_{con}-X_{o2}\\ Y_{con}-Y_{o2}\end{pmatrix}+\begin{pmatrix}X_{o2}\\ Y_{o2}\end{pmatrix} \tag{6}$$

2.2 Flow rate and its irregularity

The shaded area in Fig. 4 represents a chamber between two subsequent couples of lobe in mesh. The chamber is closed, and the movement of rotors determines the variation of its volume. When the volume increases (negative contribution to the flow rate), the pump sucks the fluid, while when the volume is decreasing (positive contribution to the flow rate), a pumping action is determined.

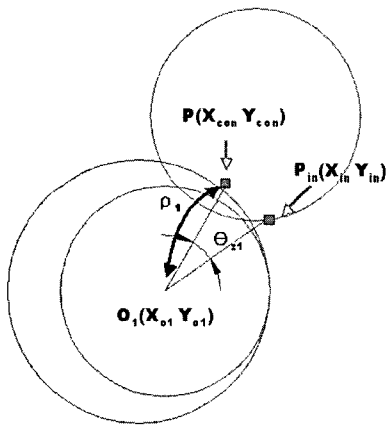

Fig. 3 Inner rotor profile tracing

The expression in Eq. (7) can be obtained by using the same principles expressed in detail in (Mimmi and Pennacchi, 1997). For the sake of brevity, only a brief explanation can be given here. Therefore it is sufficient to consider a chamber, e.g. the i-th and evaluate the contribution to the flow rate given by each flank of the rotors shown in Fig. 5. For an infinitesimal rotation and unitary axial dimension, the positive contribution is given by the areas with the sign "+", while the areas with sign "−" have to be subtracted from the previous ones. Since the areas are proportional to the square of the distance of the contact points from their respective centers, it is possible to obtain Eq. (7) by considering the relationship between the rotation of the two rotors.

$$\begin{aligned}q_i(\beta)=&\frac{1}{2}b[(|\overrightarrow{O_1A}|^2-|\overrightarrow{O_1B}|^2)\\&-(|\overrightarrow{O_2A}|^2-|\overrightarrow{O_2B}|^2)]\frac{r_2}{r_1}\omega_1\end{aligned} \tag{7}$$

Where, $\beta=\pi-(\alpha+\theta)$.

The ratio of angular velocities is directly proportional to the ratio of the lobe number and is expressed as Eq. (8).

$$\frac{\omega_1}{\omega_2}=\frac{z_2}{z_1} \tag{8}$$

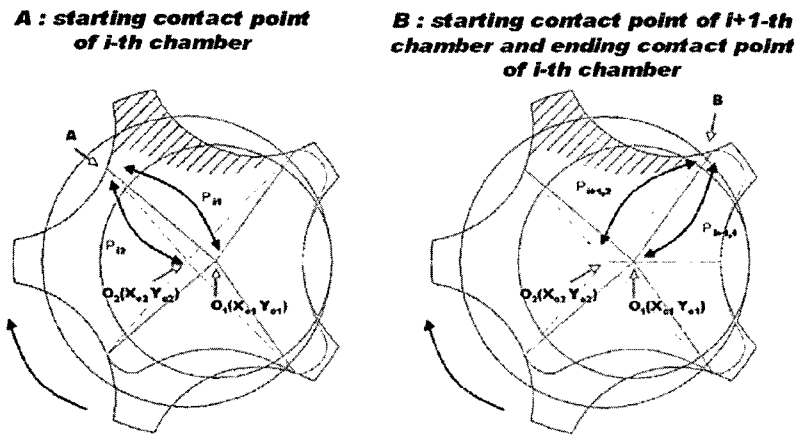

Fig. 4 Evaluation of the contribution to the flow rate given by each flank of rotors

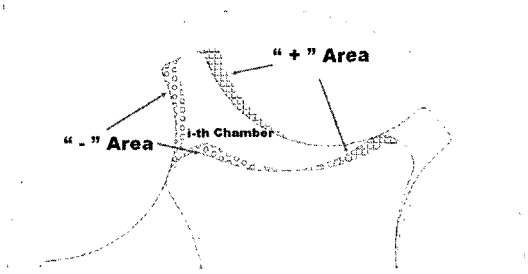

Fig. 5 Schematic diagram for the instantaneous flow rate determination

Distances that are from centers of the inner and the outer rotors to the contact points A, B of i-th chamber are expressed as Eqs. (9) and (10) in Fig. 5.

$$|\overrightarrow{O_1A}|=\rho_{i1},\ |\overrightarrow{O_2A}|=\rho_{i2},\ (\alpha=\alpha_i) \tag{9}$$

$$|\overrightarrow{O_1B}|=\rho_{i+1,1},\ |\overrightarrow{O_2B}|=\rho_{i+1,2},\ (\alpha=\alpha_{i+1}) \tag{10}$$

Where, $\alpha_{i+1}=\alpha+2\pi/z_2$.

All the chambers in the expansion phase (suction) must be connected to the intake port, in the same way that the contracting chambers are connected to the exhaust. The expression of the flow rate per revolution can be calculated as follows

$$Q=z_1\int_0^{2\pi/z_2} q(\alpha)\,d\alpha=z_1\sum_{i=1}^{2\pi/z_2} q_i \tag{11}$$

The specific flow rate (R) is defined as the ratio between the flow rate generated in a revolution and the overall volume of the pump in Eq. (12).

$$R=\frac{Q}{\pi\rho_{i,\max}^2 b} \tag{12}$$

The flow rate irregularity (i), a performance index related to noise and vibration, is expressed by Eq. (13).

$$i=\frac{q_{\max}-q_{\min}}{q_{average}} \tag{13}$$

3. Design Limitations

Before considering the flow rate determination we will think about the design limitations for the rotor. There are two important aspects in particular that limit the possibility of realizing the profiles : pressure angle, geometry.

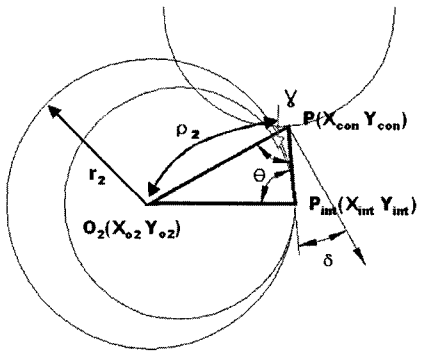

Fig. 6 Schematic diagram for pressure angle

3.1 Pressure angle

The first aspect is relative to the pressure angle between the rotors which are always ideally in mesh in z_2 points. Since the forces at contact points are proportional to the pressure angle (δ), we have to verify if the inner rotor can drive the motion with a sufficiently low pressure.

First of all we will consider the pressure angle δ in Fig. 6 as the smaller angle between the direction of the contact force on the driven rotor and the absolute velocity of the application point of the force on it. In the case that there is no friction, the pressure angle is expressed by Eq. (14).

$$\delta=\frac{\pi}{2}-\gamma \tag{14}$$

Where,

$$\gamma=\sin^{-1}\frac{r_2}{\rho_2}\sin\theta \tag{15}$$

We can plot the diagram of the pressure angle δ for a single lobe in function of the rotation angle α of the outer rotor, as is shown in Fig. 7.

The plot of Fig. 7 for each subsequent lobe is cyclically repeated with a translation of π/z_2 as shown in Fig. 8.

The pressure angle must be reduced as much as possible for the correct driving of the rotors. The diagram in Fig. 9, which reproduces the lower part of Fig. 8, shows the plot of the most favourable pressure angle δ_{opt} between the z_2 contact points on the two rotors.

Couples of rotors with reduced lobe numbers are particularly disadvantaged, since the subdivision of the diagram of Fig. 7 into a few intervals

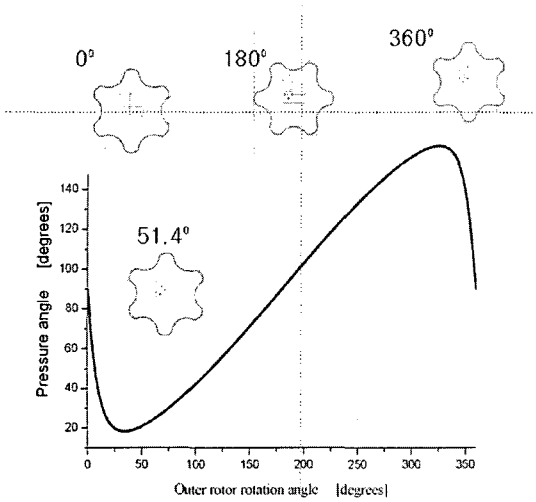

Fig. 7 Pressure angle for a single chamber

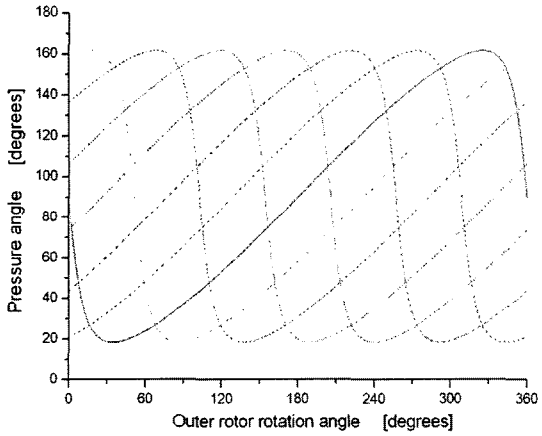

Fig. 8 Pressure angle for all the chambers

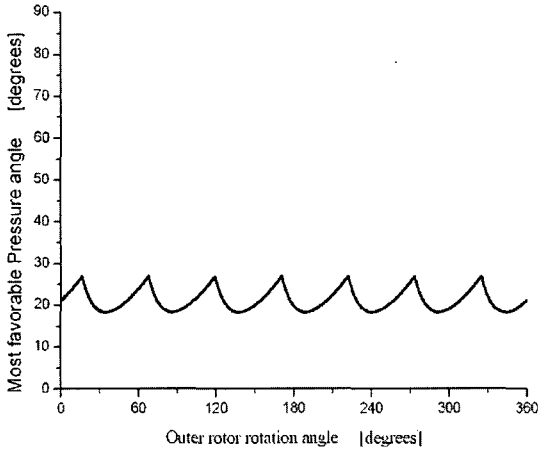

Fig. 9 Schematic reference for the instantaneous flow rate determination

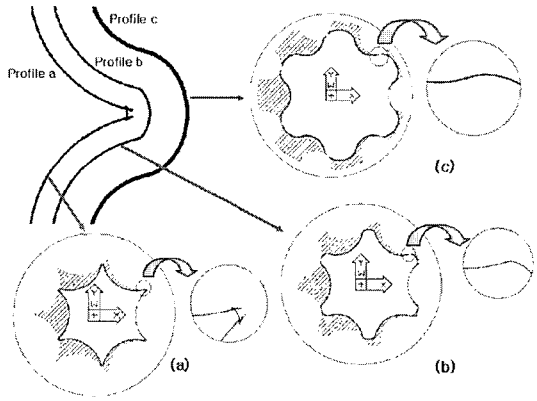

Fig. 10 Theoretical inner rotor profiles

can determine the impossibility of δ_{opt} reaching a value lower than an acceptable value.

3.2 Geometry

The second aspect is relative to the geometry that limits the possibility of realizing the profiles. The conjugated profile, generated by the outer rotor, although analytically acceptable, is not feasible, if it presents cusps (Fig. 10(b), profile b) or loops (Fig. 10(c), profile c).

The profile is correct as far as r_{t2} is lower than r_{t2max} as shown in Fig. 10(a). The limit value that produces sharp points or cusps is $r_{t2}=r_{t2max}$. The condition $r_{t2}>r_{t2max}$ produces undercutting as shown in Fig. 10(c). Even if in that case the procedure to determine the conjugate profile is quite different, the criterion can be also applied here since it is based only on design parameters. Therefore the value of r_{t2max} is given by Eq. (16) (Mimmi and Pennacchi, 1997; Beard et al., 1991).

$$r_{t2,max}=\frac{\sqrt{3^3}\sqrt{z_1(d-r_2^2)}}{\sqrt{(z_2+1)^3}} \tag{16}$$

4. Design Optimization

The optimum design parameters for the gerotor are obtained by fixing the lobe numbers z_1 and z_2, by varying r_{t2} and d in a suitable range and by finding those that maximize the flow rate and minimize its irregularity and specific slipping.

By using the same values for z_1, z_2, r_{t2} and d and by varying d/e and r_{t2}/e it is possible to find the parameter value that maximize the flow rate and minimize its irregularity for the gerotor.

The order of priority of the objective functions, having influence on efficiency of the pump, was obtained from the interviews with workers in an actual field, and is as follows;

(1) Flow rate and flow rate irregularity
(2) Specific slipping

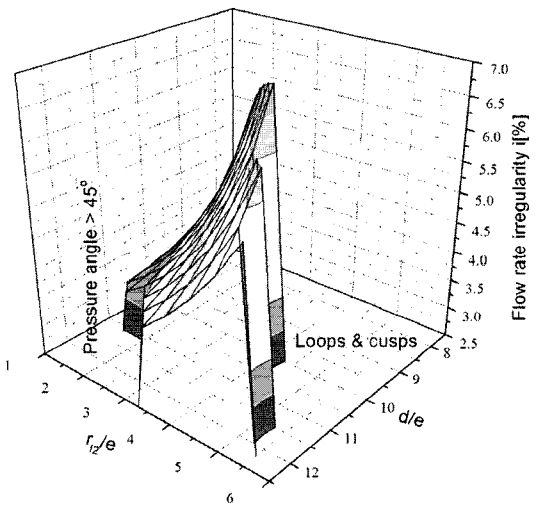

Fig. 11 Specific flow rate diagram for $z_1=6$, $z_2=7$

4.1 The flow rate and its irregularity

When the lobe numbers are 6/7, the diagrams obtained are similar to those reported in Figs. 11 and 12.

These figures show the flow rate irregularity and specific flow rate in which the lower left part, high values of the difference; $d-r_{t2}$, is eliminated due to unacceptable δ_{opt} values. In fact, for these d/e and r_{t2}/e values, δ_{opt} during the mesh reaches values greater than 45°. Similarly the upper right part of Figs. 11 and 12, lower values of the difference; $d-r_{t2}$, is eliminated because of loops and cusps in the profiles of the inner rotor.

By observing Figs. 11 and 12, some considerations can be made. The first is that specific flow rate strongly depends on the difference $d/e-r_{t2}/e$ and decreases when this increases. This trend is exactly the same whether z_1 is odd or even. When z_1 is odd and z_2 even in Fig. 13, the flow rate irregularity decreases when the flow rate increases. So the couple which obtains the best specific flow rate also gives the lowest flow rate irregularity. When z_1 is even and z_2 is odd in Fig. 12, the flow rate irregularity always decreases when r_{t2}/d decreases. In this case the couples which obtain the best specific flow rate do not obtain the lowest flow rate irregularity.

Table 1 shows the configurations that obtain the best performance; for z_1 even and z_2 odd we

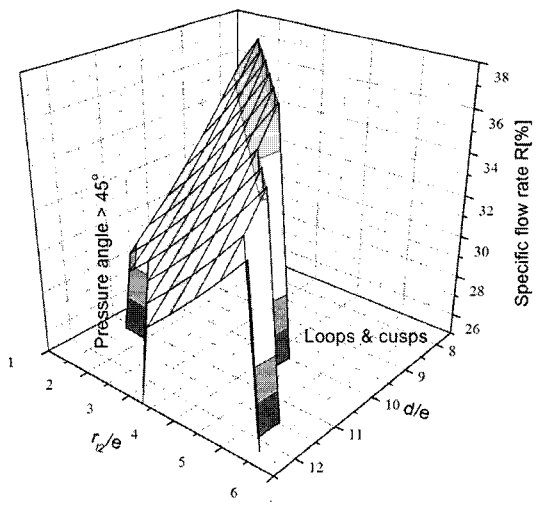

Fig. 12 Flow rate irregularity diagram for $z_1=6$, $z_2=7$

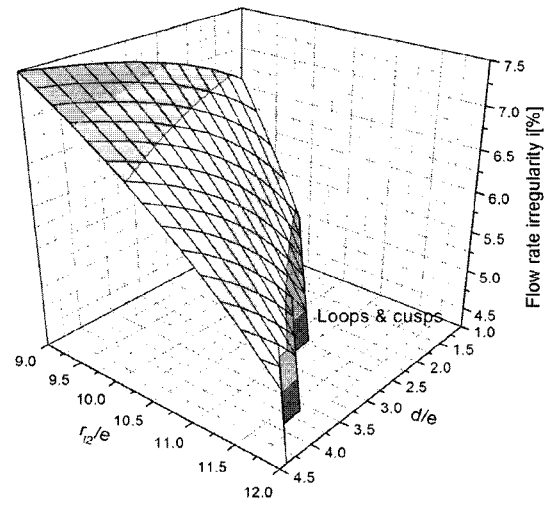

Fig. 13 Flow rate irregularity diagram for $z_1=7$, $z_2=8$

have selected the couples which give the best compromise between specific flow rate and its irregularity.

From the analysis of the data in Table 1 it is possible to observe that the specific flow rate decreases as much as the lobe number increases, while the behavior is the opposite for the flow rate irregularity that drastically decreases.

4.2 The specific slipping

The design optimization of profile in the gerotor needs another performance index, the specific slipping, in addition to the flow rate and its irregularity. It is important to limit the wear as much as possible because they can not be recovered as occurs in involute gears when the profiles of rotors meshing in z_2 points are worn out. For this reason it is important to minimize the specific slipping.

Figure 14 shows the maximum specific slipping of the rotors when $d/e-r_{i2}/e$ assumes equal values.

The specific slipping for the inner rotor is expressed as follows

$$S.S.=\frac{|s_2-s_1|}{s_2} \tag{17}$$

In the Eq. (17) s_1 and s_2 are the displacement of the contact point along the inner and outer rotor profile for a generic rotation. The specific slipping of the inner rotor is finite because the contact point always moves along its profile in the same direction and s_1 never becomes equal to zero.

Table 1 Best configurations

Z_1	Z_2	r_{i2}/e	d/e	R [%]	i [%]
3	4	3.5	6.0	47.43	19.77
4	5	2.0	6.0	42.90	12.18
5	6	3.5	8.5	39.67	9.02
6	7	2.5	8.5	36.87	6.16
7	8	3.0	10.0	33.62	4.87
8	9	2.5	10.5	31.68	3.59
9	10	3.5	13.0	27.63	3.41
10	11	3.0	13.5	26.67	2.15
11	12	2.5	14.0	25.30	2.16
12	13	2.5	15.0	23.06	1.35
13	14	2.0	15.5	22.36	1.67

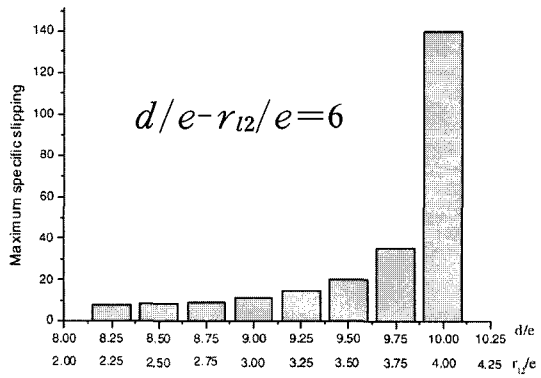

Fig. 14 Maximum Specific slipping according to the same values of $d/e-r_{i2}/e$

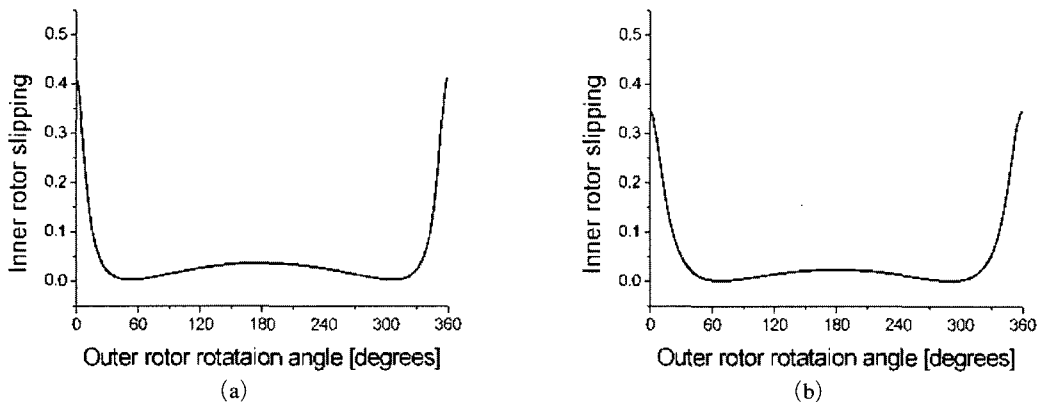

Fig. 15 The slipping distances regarding the lobe shapes of the inner rotor in Fig. 14

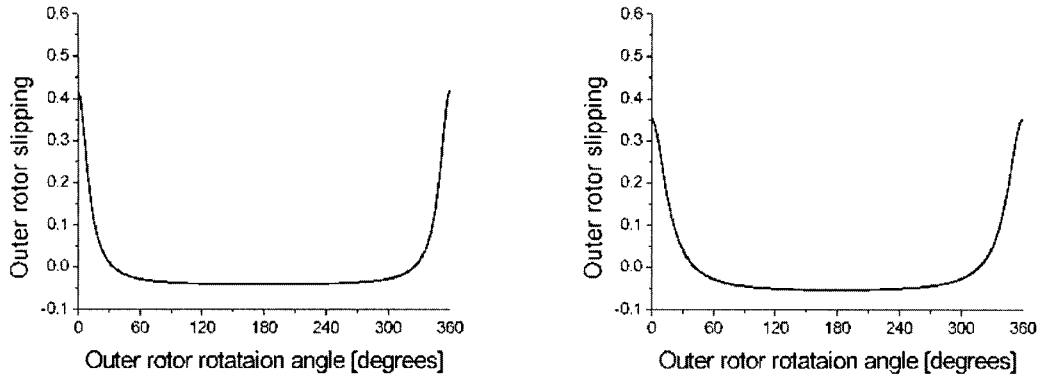

Fig. 16 The slipping distances regarding the lobe shapes of the outer rotor in Fig. 14

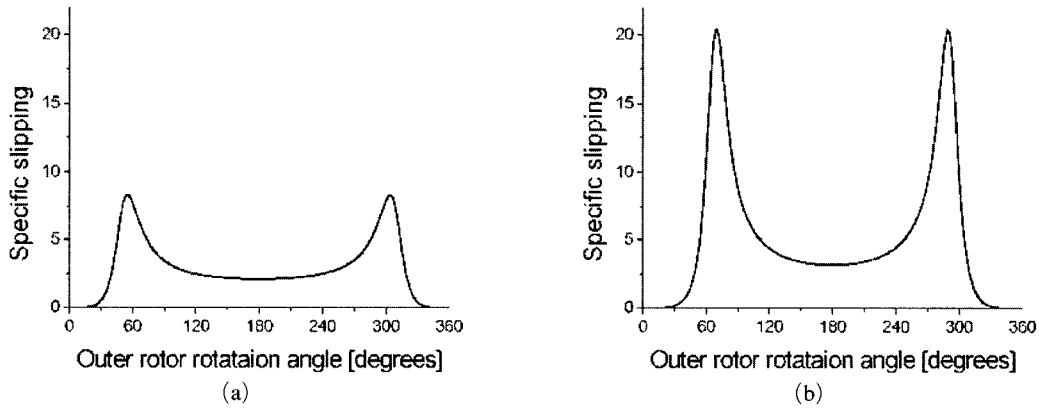

Fig. 17 Inner rotor specific slipping regarding the lobe shapes of the outer rotor in Fig. 14

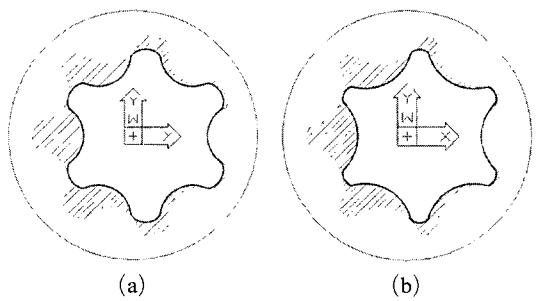

Fig. 18 Pump with same lobe numbers but different ratio d/r_{i2}

The displacements of the inner and the outer rotors regarding the values, $d/e=8.25$ and $r_{i2}/e=2.25$: $d/e=9.50$ and $r_{i2}/e=3.50$, shown in Fig. 14 for a generic rotation were shown in Figs. 15 and 16. The inner rotor specific slipping, given by the formula Eq. (17), is shown in Fig. 17. The two pumps in Fig. 18 have similar performances in terms of specific flow rate, since d/e-r_{i2}/e assumes equal values; nevertheless they have a different specific slipping of the contact point along the rotor contours. Fig. 18(a) shows the best rotor with the minimum specific slipping obtained from the design optimization.

5. Conclusion

This study has carried out a geometrical and kinematic analysis considering design variables and design limits of the outer rotor with a circular lobe shape.

(1) The closed-form parametric equations for the inner and outer rotor with a circular lobe shape were suggested by a new approach.

(2) The suitable range that does not present cusps or loops and that obtains the lowest press

angle was found from a geometrical point of view.

(3) The optimal design parameters were obtained by fixing the lobe numbers and calculating flow rate and flow rate irregularity according to d/e and r_{12}/e.

(4) If the inner rotor lobe number is odd, the design parameter sets that minimize the flow rate irregularity also maximize the specific flow rate. If even, the design parameter sets that optimize the two performance indexes are different.

(5) A suitable choice of the design parameters can improve the specific slipping of the inner rotor.

References

Beard, J. E., Hall, A. S. and Soedel, W., 1991, "Comparison of Hypotrochoidal and Epitrochoidal Gerotors," *ASME Journal of Mechanical Design*, Vol. 113, pp. 133~141.

Choi, J. C., Kim Chul, Kim, J. H. and Kim, Y. M., 2002a, "Development of a system for progressive working of electric product by using Fuzzy Set Theory," *International Journal Advanced Manufacturing Technology*, Vol. 20, No. 10, pp. 765~779.

Choi, J. C., Kim Chul and Kim, J. H., 2002b, "A Study of the Progressive working of an Electric Product Using a 3D Shape Recognition Method," *International Journal Advanced Manufacturing Technology*, Vol. 19, No. 7, pp. 525~536.

Colbourne, J. R., 1975, "Gear Shape and Theoretical Flow Rate in Inner Gear Pumps," *Transactions of the CSME*, Vol. 3, No. 4, pp. 215~223.

Kim, J. H. and Kim Chul, 2006, "Development of an Integrated System for Automated Design of Gerotor Oil Pump," *KSPE*, Vol. 23, No. 2, pp. 88~96.

Mimmi, G. and Pennacchi, P., 1997, "Inner Lobe Pump Design," *Transactioins of the CSME*, Vol. 21, No. 2, pp. 109~121.

Saegusa, Y., Urashima, K., Sugimoto, M., Onoda, M. and Koiso, T., 0000, "Development of Oil-Pump Rotors with a Trochoidal Tooth Shape," *SAE Paper* No. 840454.

Shim, J. Y., Kwak, J. S. and Song J. B., 2000, "Development of an Optimal Design Program for the Helical Gear on Vehicle Transmission," *Journal of the KSPE*, Vol. 17, No. 11, pp. 88~93.

Tsay, C. B. and Yu, C. Y., 1989, "Mathematical Model for the Profile of Gerotor Pumps," *J. CSME*, Vol. 10, No. 1, pp. 41~47.

Yu, C. Y. and Tsay, C. B., 1990, "The Mathematical Model of Gerotor Pump Applicable to Its Characteristic Study," *J. CSME*, Vol. 11, No. 4, pp. 385~391.